Int J Adv Manuf Technol (2012) 60:101–110
DOI 10.1007/s00170-011-3609-7

ORIGINAL ARTICLE

Numerical simulation and metal flow analysis of hot extrusion process for a complex hollow aluminum profile

Cunsheng Zhang · Guoqun Zhao · Hao Chen · Yanjin Guan · Fujun Kou

Received: 5 July 2010 / Accepted: 23 August 2011 / Published online: 1 September 2011

Abstract The most important way to improve the quality of aluminum profiles is to assure the material flow through die land exit with the same velocity. In this paper, a numerical model was developed to investigate metal flow behavior during aluminum profile extrusion. Firstly, the numerical model for a complex hollow aluminum profile was built based on the arbitrary Lagrangian–Eulerian program HyperXtrude. Then, with the numerical model, metal flow behavior at each stage during the whole extrusion process was analyzed and dead zones in the die cavity were also investigated by means of the particle tracking method. Finally, the numerical results were validated by comparing with the nose ends of two extrudates in practice, and the comparison showed that the numerical model developed in this work could provide the effective guidance for practical production.

Keywords Aluminum profile extrusion · Metal flow analysis · HyperXtrude

1 Introduction

The extrusion process is an attractive production method in industry because of its ability to achieve energy and material savings, quality improvement and development of homogeneous properties throughout the component. Lightweight construction, especially in the area of transportation engineering, is of increasing significance even with decreasing numbers of pieces [1, 2].

During the profile extrusion process, an understanding of the metal flow in porthole die cavity is important because it is response to the design of die structure and selection of process parameters. Usually, aluminum profile extrusion is a very complex process of metal flow, which is mainly dependent on the level of the die design. If the flow velocity in the cross-section of the bearing exit is non-uniform, defects such as twist, wave, bend, and crack will emerge in the extrudate and even the die will be spoiled. Yet current design of extrusion die structure in extrusion enterprises is primarily based on the trial-and-error method. The performance of the dies to a large extent is determined by the experience of die designers. With this kind of design pattern, it is impossible to guarantee product quality and productivity when the profile structure is more complex and actual production has to be stopped or postponed.

With increasing application of computational techniques in recent years, a large number of studies on the numerical simulation of extrusion process have been carried out to improve the product quality and production efficiency. These numerical models are used to predict die stresses, temperature distribution, stress and strain gradients of the extrudate, flow velocities, extrusion pressures, dimensions, and distortions, etc., which are difficult to measure by traditional means. In addition, the effects of die design features and process parameters on these variables can be readily and efficiently evaluated to optimize both die design and process parameters.

Yang et al. developed the rigid viscoplastic finite element programs for analyzing extrusion process, and the

C. Zhang · G. Zhao (✉) · H. Chen · Y. Guan
Key Laboratory for Liquid–Solid Structural Evolution and Processing of Materials (Ministry of Education),
Shandong University,
Jinan, Shandong 250061, People's Republic of China
e-mail: zhaogq@sdu.edu.cn

F. Kou
CSR Qingdao Sifang Co., Ltd,
Qingdao, Shandong 266111, People's Republic of China

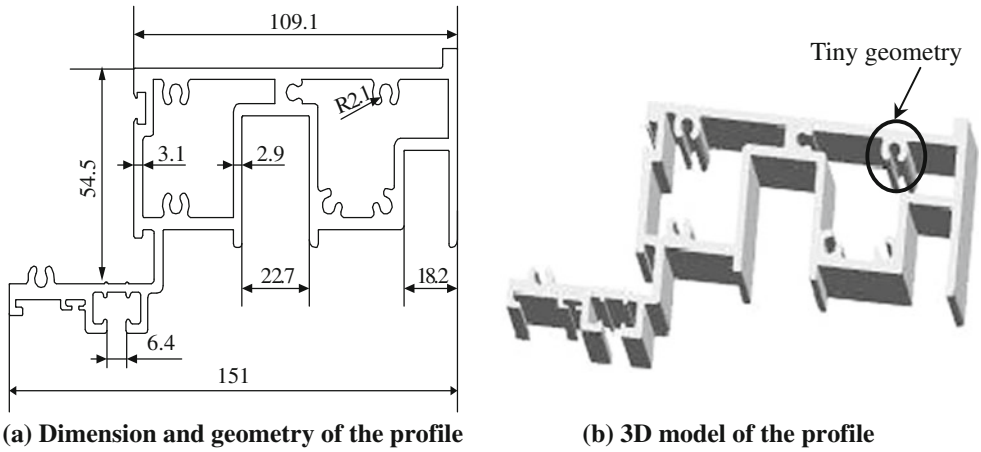

Fig. 1 2D and 3D geometry of the profile studied in this work

(a) Dimension and geometry of the profile **(b) 3D model of the profile**

effects of flow guide, die lands, and portholes on the metal flow during the extrusion process have been investigated [3]. Lof and Blokhuis have presented a method for the simulation of the extrusion of complex profiles with an arbitrary Lagrangian–Eulerian (ALE) code DiekA. The method was demonstrated for a particular die and the results were compared to those obtained in practice [4]. Li et al. used Lagrangian-based 3-D software to model metal flow through a die and to evaluate the effect of die design features on dimensional distortions [5]. Lee et al. have described a 3D finite element method simulation of porthole die extrusion process for producing condenser tubes used for a cooling system of automobiles. The effects of chamber shape on the material flow, welding pressure, extrusion load, and the tendency of mandrel deflection have been evaluated [6]. Wu et al. simulated the extrusion process of an AA1100 rectangular hollow pipe using finite volume method software Msc/SuperForge. An optimal die design scheme was determined and it was found that the path shape from the portholes to the bearing entrance was an important parameter in flat porthole die design [7]. Kim investigated the lubrication effect on the backward extrusion of thin-walled rectangular aluminum case with large aspect ratio using Superforge [8]. Liu et al. have conducted a detailed analysis of metal flow into a porthole extrusion die to produce a thin-walled square magnesium tube by means of Deform-3D in both the transient state and steady state [9]. Fang et al. investigated the effect of steps in the die pocket on metal flow to produce two chevron profiles with unequal thicknesses through two-hole dies, by means of Deform-3D simulation of extrusion in the transient state [10]. They also studied the effects of die bearing and ram speed on extrudate temperature, dimensional precision, surface quality, and extrusion pressure during a typical industrial profile extrusion process [11]. Bastani et al. performed a transient simulation of the aluminum extrusion process based on Altair HyperXtrude 9.0 in order to study how process parameters influence flow balance and exit temperature. The influence of billet taper, front billet temperature, and ram speed on the run-out velocity and temperature of two separate outlets was investigated [12]. In the optimization of die structure and process parameters, choosing the forming energy consumption and the maximization of the possible area reduction as the optimization

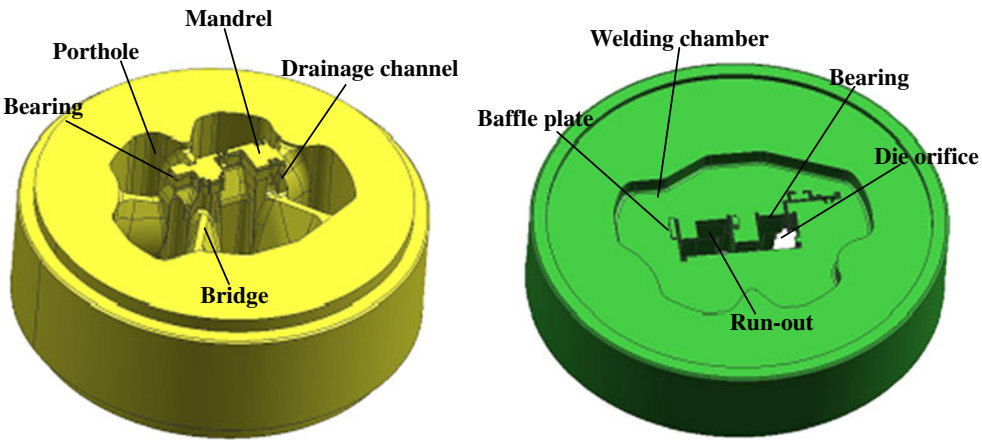

Fig. 2 Extrusion die designed in this work

(a) Upper die **(b) Lower die**

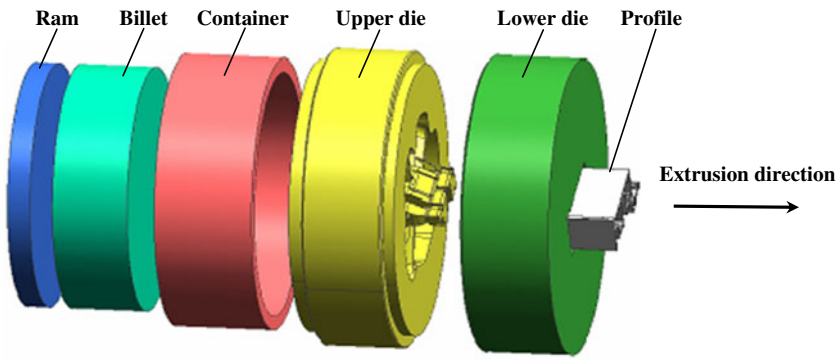

Fig. 3 Structure components of a profile extrusion die

objectives, Mihelic and Stok applied the finite element discretization and nonlinear mathematical programming techniques to optimize the extrusion tools [13]. Ulysse adopted the finite element method combining with optimization techniques to determine the optimal bearing length. The numerical accuracy has been verified using published experimental data for a two-out extrusion die with bearings [14]. Zou et al. presented an improved optimal design method for hot extrusion die using updated sequential quadratic programming method and the results had been validated by real experiment [15]. Byon and Hwang proposed a process optimal design methodology applicable to cold and hot forming on the basis of an integrated thermomechanical finite element process model and a derivative-based optimization scheme. It was demonstrated through their investigation that the approach was effective in revealing the effect of strain hardening and heat transfer on the predicted optimal die shape in cold and hot extrusion, respectively [16]. Chen et al. proposed a computer-aided engineering/computer-aided optimization model based on finite volume method, artificial neural network, and genetic algorithm to optimize extrusion process parameters and die structure [17].

In the past, numerical simulations of aluminum profile extrusion have been limited to relatively simple solid rods and strips or axisymmetric tubes and low extrusion ratios, and the analysis of complex hollow profiles has not much been presented so far. Moreover, the simulations of extrusion process are mainly based on Lagrangian or Eulerian method in the current papers, but both of which have drawbacks. Yet the ALE algorithm alleviates many of the drawbacks that the traditional Lagrangian- and Eulerian-based finite element simulations have, and can be used to perform comprehensive engineering simulations, including heat transfer, fluid flow, fluid–structure interactions, and metal manufacturing [18]. In this paper, the ALE program HyperXtrude has applied to model an extrusion process for a complex hollow aluminum profile with thermal coupling between the tools and material. The determinations of mesh size, boundary conditions and process parameters, etc. were described in detail. Based on the numerical model, the metal flow behavior at each stage during the whole extrusion process was analyzed and dead zones were investigated by particle tracking function provided by HyperXtrude. To validate the numerical method, the comparison with two practical extrudates was finally given.

2 Modeling of extrusion process with HyperXtrude

2.1 Die structure and geometry

Figure 1 shows the main dimension and geometry, and 3D model of the product in the present study. The profile section is complex with two cavities and many tiny geometry features as shown in Fig. 1 (unit, millimeter).

In this work, a porthole die is designed for the production of this profile, which is shown in Fig. 2. A flat porthole die is mainly composed of four parts: an upper die, a lower die, location pins, and coupling bolts. The upper die has portholes, port bridges, and two die mandrels as illustrated in Fig. 2a. A porthole is a channel through which material flows into a die orifice. In this case, five portholes are adopted in the upper die in order to allocate

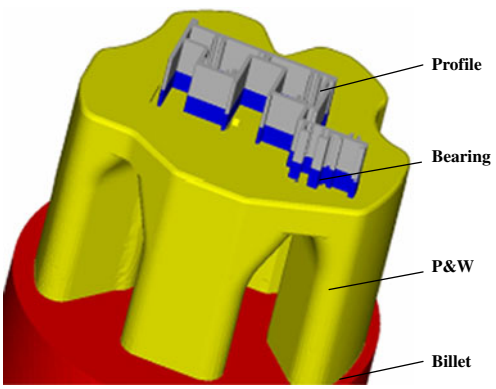

Fig. 4 Material domains in different extrusion zones

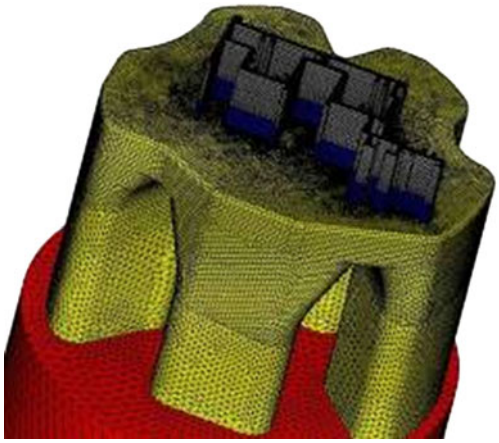

Fig. 5 Mesh generation of whole numerical model

material rationally and balance the metal flow. Die mandrels are used to form the inner contour of a profile. A port bridge is a bracket supporting the die mandrels, and here sank port bridges are applied to improve the weld quality. Meanwhile, drainage channels are introduced on die mandrels to guide the material flowing into the parts which are difficult to form, such as tiny geometries of the profile shown in Fig. 1b.

The lower die has a welding chamber, a die orifice, and a run-out as illustrated in Fig. 2b. A welding chamber is used to collect the material flowing through the portholes and weld them into an integral body. The material in the welding chamber gradually accumulates and the inner hydropressure increases until it flows out of the die orifice. Besides, there is a die bearing land in the upper and lower dies as illustrated in Fig. 2a and b, respectively. The bearing land of the die orifices determines the outer shape and dimensions of the extrudate and adjusts the material flow. From Fig. 2b, two baffle plates in the welding chamber are adopted to increase the resistance of metal flow in the parts where metal flows faster than other parts. When the material encounters the baffle plates, the direction of the metal flow is changed and the metal is forced to flow into the parts with relatively small frictional resistance. In addition, a run-out in the lower die is used to support the die bearing during the extrusion process and to keep away from scratching of the extrudate until it goes through the die exit successfully.

The location pins and coupling bolts are used to couple and fix the upper and lower dies together. The material flows through the inner space between the die orifice and die mandrels and forms a profile. Figure 3 shows the structure components of the profile extrusion dies. For simplification, the thinner parts, such as the bolt holes, which are not relevant with simulation, can be omitted in the numerical models. The dies can be modeled with 3D modeling software UG and imported to HyperXtrude in IGES or STEP formats.

2.2 Mesh generation of whole numerical model

To simulate the extrusion process with HyperXtrude, all the domains that material flows through should be extracted and meshed. After importing the 3D models of the extrusion dies into HyperXtrude, it is necessary to manually clean up the tiny entities in the die geometry that influence the size and quality of mesh generating in the following procedure. Being convenient for creating boundary conditions and meshing, the model is divided into five parts: billet, porthole, welding chamber, bearing, and profile. For the sake of simplicity, here portholes and the welding chamber are merged into one part (noted as P&W), as shown in Fig. 4.

In addition, element size influences the simulation accuracy and time cost. Smaller element size implies large amounts of elements and higher simulation accuracy but longer simulation time. Considering the extruded complex hollow profile is relatively thinner, the elements in the bearing area should be smaller. Fortunately, it is permitted to set different element sizes and types at different domains within the whole model in HyperXtrude. Here, triangular prism element is adopted in the part of bearing and profile, and tetrahedral element is used in other parts. In order to control the element number and ensure also calculation accuracy, varying mesh density within the whole model is adopted in accordance with the extent of local deformation. In the whole extrusion process, the region near the die bearing will undergo severe shear deformation because the final shape of the profile is formed in the die bearing. Thus, in the regions of bearing and profile, finer meshes are assigned, and four layers of element are meshed. While only upsetting deformation occurs in other regions, relatively coarse meshes are used. The meshes of the billet,

Table 1 Material properties of AA6063 and H13

	Young's modulus/Pa	Poisson's ratio	Density/ (Kg × m^3)	Thermal conductivity/ $[N/(s \times ^\circ C)]$	Specify heat/ $[N/(mm^2 \times ^\circ C)]$
AA6063	4.0E+10	0.35	2,700	180	896
H13	2.1E+11	0.35	7,870	24.3	460

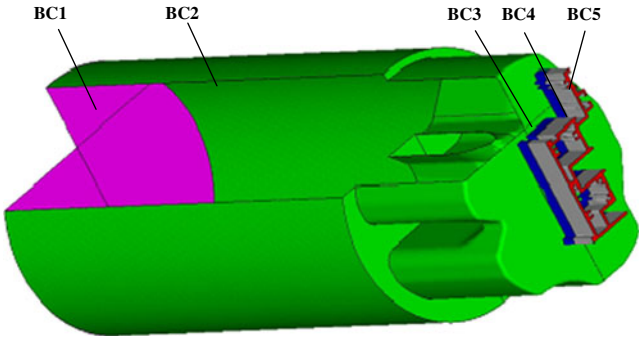

Fig. 6 Boundary conditions used in this extrusion process

porthole, welding chamber, and profile are shown in Fig. 5 and the mesh number of the whole model is about 688,000.

2.3 Definition of material parameters

Constitutive equations are often employed to mathematically determine flow stress as a function of parameters such as strain, strain rate, temperature, and so on. One such constitutive equation used in aluminum profile extrusion is typically referred to as the Sellars–Tegart model [4], is:

$$\sigma = \frac{1}{\beta}\sinh^{-1}\left(\frac{Z}{A}\right)^{1/n} \tag{1}$$

Where σ is the flow stress, β, n, and A are the temperature-independent material parameters, and Z is the Zener–Hollomon parameter, defined by:

$$Z = \dot{\bar{\varepsilon}} e^{Q/\mathrm{RT}} \tag{2}$$

Where $\dot{\bar{\varepsilon}}$ is the effective strain rate, Q is the activation energy, R is the universal gas constant, and T is the absolute temperature. Parameters values used for AA6063 in this work are as follows [19]: $Q = 1.416 \times 10^5 \mathrm{J/mol}$, $R = 8.314 J/(\mathrm{mol} \times k)$, $A = 5.91 \times 10^9 s^{-1}$, $n = 5.385$, $\beta = 4 \times 10^{-8} m^2/N$.

The die material is chosen as H13 steel with good abrasion resistance, hot hardness, and low sensitivity to heat checking, which can be subjected to drastic heating and cooling at high operating temperatures. The mechanical properties of H13 and A6063 are given in Table 1.

2.4 Definition of boundary conditions

Ideal extrusion process is that required to bring about homogeneous deformation in producing the profile. In practice, it is not possible to achieve a situation of ideal or homogeneous deformation in extrusion due to the contributions of inhomogeneous deformation and friction. As a result of strong adhesion of hot aluminum to the extrusion tooling made of tool steel, the friction between the billet and container is large. For the sake of convenience, the sticking condition is used for all of the interfaces between the billet and the tooling (container and die) except at the die bearing land where fully slip friction conditions are applied on the surfaces in contact with the bearing. Because profile extrusion processes usually involve a high contact pressure, it is generally more appropriate to use the law of constant plastic shear friction. A friction factor of 0.3 was prescribed so as to simplify the complex interfacial conditions ranging from full sticking at the die entrance to slipping at the end of the bearing.

HyperXtrude 10.0 supports ten types of boundary conditions in order to distinguish different boundaries where the material flows through different extrusion zones. Each type of boundary condition corresponds to the related parameters. In this work, five types of boundary conditions are applied as described by different colors in Fig. 6, and the corresponding boundary conditions are listed in Table 2.

2.5 Other process parameters

Once the boundary conditions have been set up and assigned, the process parameters should be defined. The process parameters are determined based on the experience of practical production. The billet is a cylinder with the initial diameter of 180 mm and the length of

Table 2 Boundary conditions used in this extrusion process

BC No.	Type	Acting objects	BC parameters to be defined	Color
BC1	Inflow	Billet-DummyBlock	Ram speed:1.0 mm/s Initial temp. of billet: 480°C	Pink
BC2	Solidwall	Billet-container; Billet-die; Porthole-Die	Fully sticky friction condition Initial temp. of tool: 460°C Heat convection coefficient: 3000 $\mathrm{W/m^2} \times^\circ \mathrm{C}$	Green
BC3	Bearing	Bearing-die	Slipping friction condition with a factor of 0.3	Blue
BC4	Freesurface	Freesurface	Normal velocity on surface: 0	Gray
BC5	Outflow	Exit	Pressure: 0	Red

BC boundary condition

Table 3 Process parameters used in simulation

Billet diameter/mm	Billet length/mm	Extrusion ratio	Initial temperature of billet/°C	Initial temperature of tool/°C	Heat convection coefficient/ ($W/m^2 \times^\circ C$)	Ram speed/ (mm/s)
180	360	16.9	480	460	3,000	0.1

360 mm, and the calculated extrusion ratio is 16.9. The initial temperature of the billet and the tools (including dies and container) are 480°C and 460°C, respectively. The velocity of extrusion stem is 0.1 mm/s. The heat convection coefficient between the die and billet material is 3,000 $W/m^2 \times °C$. The process parameters used in simulation are given in Table 3.

3 Metal flow analysis of whole extrusion process

The simulation of the aluminum profile extrusion takes almost 4 h of central processing unit time on a Linux workstation with 16 GB of RAM and four 3.16 GHz Intel Xeon processors to obtain a stationary solution for the model described above. A large variety of results can be obtained from the numerical simulation such as velocities, strains, stresses, temperatures, and extrusion forces, etc. Here, to analyze metal flow during the extrusion process, what interests us particularly is the metal flow velocity at each stage of extrusion because it is important to see the exit velocity of the profile over the cross-section of the profile in order to judge whether this die will perform adequately in practice. Figure 7 shows the velocity distribution at the die exit obtained by the above numerical simulation. It gives an indication of how the nose end of the profile will look. From this figure, a large difference in metal velocity at the cross-section of the extrudate is observed. Part 1 of extrudate has a relative low exit velocity (19.20 mm/s) compared to the other parts, especially in parts 2 and 3, where maximum velocity (40.83 mm/s) is located in Fig. 7. Due to a large non-uniformity of velocity distribution, a severe twist deformation in part 1 occurs, which will be validated in the following experiments.

3.1 Metal flow through the porthole die

Figure 8 shows the velocity distribution of the nine cross-sections extracted from the inlet of the portholes to the bottom of the welding chamber along the extrusion direction, which reflects the status of the metal flow in the whole extrusion process.

Figure 8a shows the velocity distribution at the entrance of the portholes. The contour drawn on the figure shows the velocity scalar value on this specified surface normal to the extruding direction (red and blue represents the maximum and minimum velocity values, respectively; the same as below). From Fig. 8a, it is seen that metal flows faster in the center than that at the periphery for every porthole. This phenomenon is caused by the friction (sticky condition) on the porthole wall. Moreover, metal flows faster in the portholes 3 and 4 than in the portholes 1 and 2, which leads to a larger velocity in parts 2 and 3 than that in part 1, the same tendency could be observed in Fig. 7.

Figure 8b shows the metal flow status in the portholes. Compared with Fig. 8a, a decreasing velocity gradient in each porthole is found, which is also due to the increasing frictional resistance between the billet material and the porthole wall. The strong friction on the porthole wall prevents the surface part of the billet from flowing to the

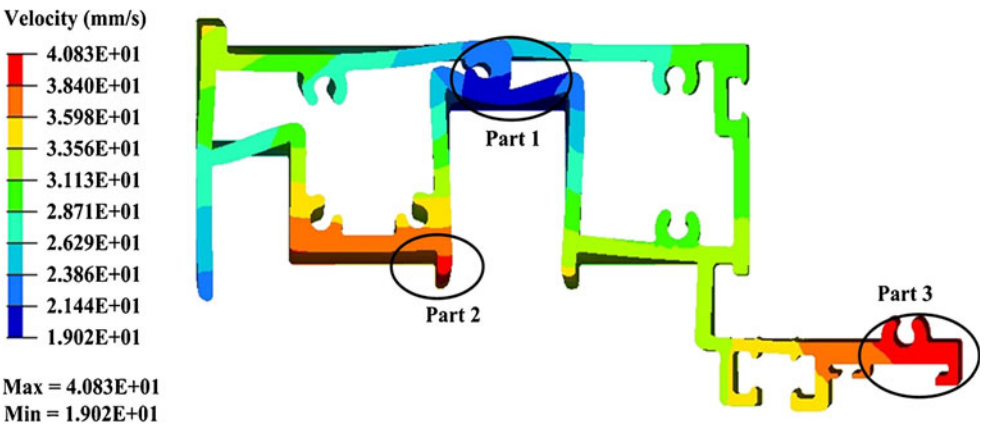

Fig. 7 Velocity distribution at the cross-section of the extrudate

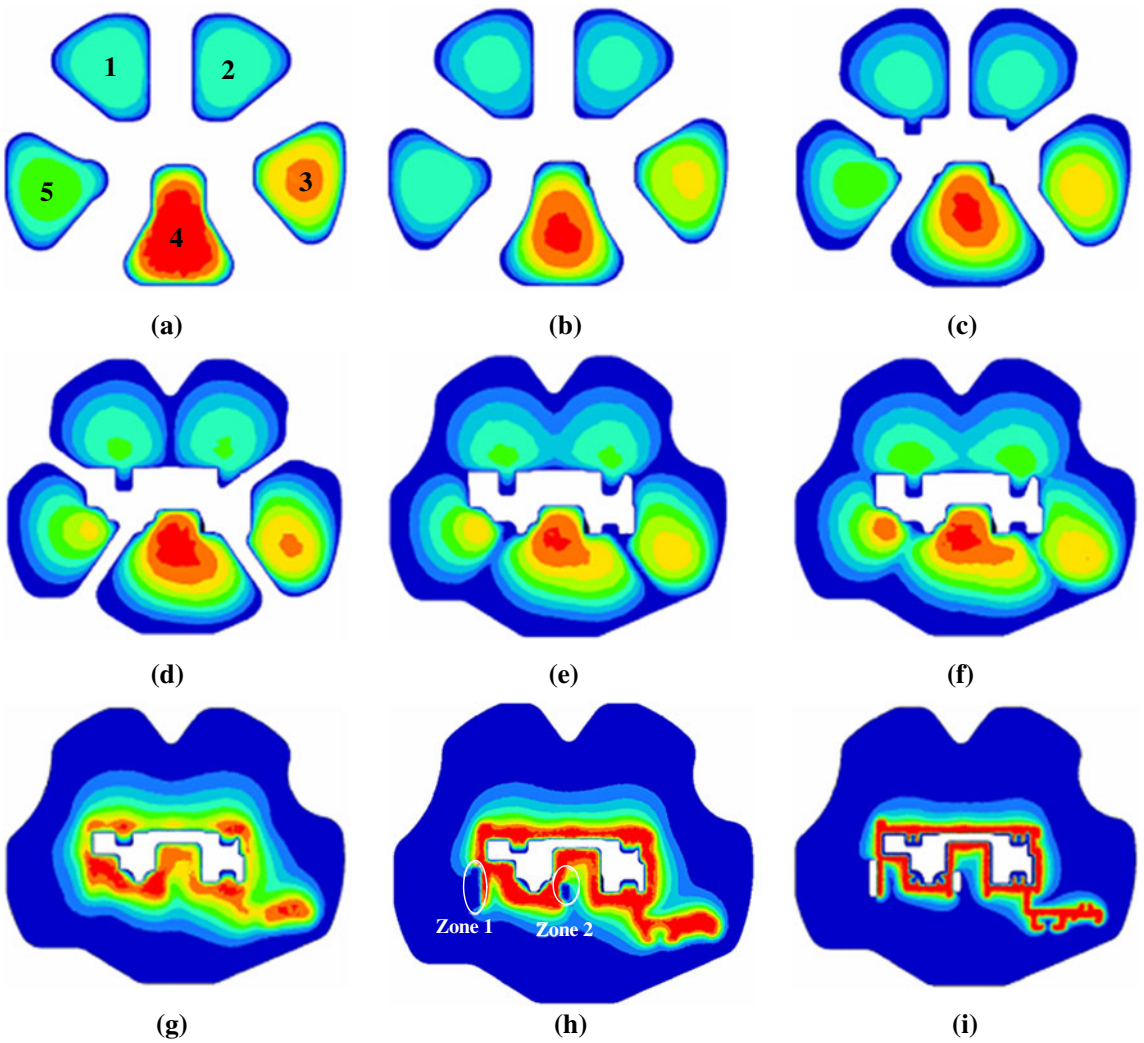

Fig. 8 Metal flow at different stages in the extrusion process

extruding direction. As a consequence, a radially slower velocity distribution towards the center of porthole is shown, as reported in the previous study [20].

Figure 8c shows the velocity distribution at the inlet of the drainage channel. One part of the material continues to flow into the die orifice along the extrusion direction, while the other flows into the tiny geometries (in Fig. 1b) along the drainage channel. Thus, enough material flows into the drainage channel to supply for tiny geometries of the profile which are difficult to form.

Figure 8d shows that the metal begins to reweld in the welding chamber between portholes 1 and 2, which is caused by a relatively deeper-sank bridge here than other regions. Thus, much more material is located here in order to supply for part 1 of the extrudate even though it is seen that part 1 of the extrudate has a relatively low metal flow velocity from Fig. 7.

Figure 8e shows that metal in all portholes begins to reweld. Material out of portholes 1 and 2 rewelds faster than that in other portholes, moreover, it is seen that a dead zone with a nearly zero velocity is located under the bridges between portholes 1 and 5, portholes 2 and 3, portholes 3

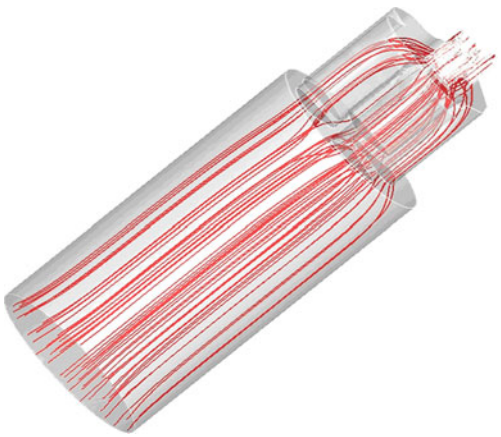

Fig. 9 Metal flow analysis by means of particle tracking

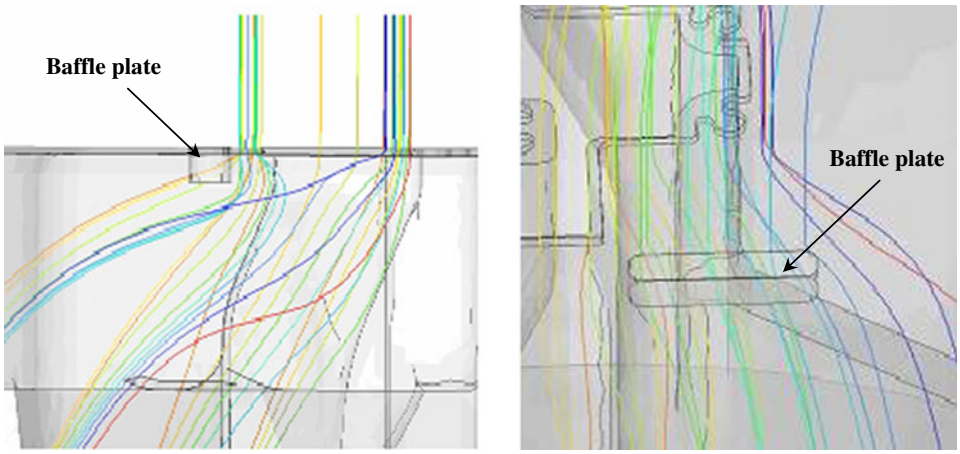

Fig. 10 Metal flow near baffle plates with particle tracking

and 4. That is to see, part of material has not been completely rewelded.

Figure 8f shows the status of the metal flow in the welding chamber. It can be seen that metal under the bridges are rewelded further and metal flow in the welding chamber tends to be uniform.

Figure 8g shows a nearly finished rewelding process. All material in the welding chamber is accumulated together. From this moment on, metal begins to concentrate near the die orifice, consequently, it can be seen that metal under the die orifice flows significantly faster than that near die mandrels and the corner of the welding chamber.

Compared to Fig. 8g, two zones (zones 1 and 2) with relatively lower velocity appears in Fig. 8h, which is identified by white circles. This is caused by baffle plates designed in the welding chamber in order to increase the frictional resistance and make metal flow to other zones.

Figure 8i shows the velocity distribution at the inlet of the die orifice, at this moment the velocity reaches the peak. The metal flow at the exit of the die is regulated by the bearing land and the final shape of the extrudate is gained.

3.2 Metal flow in local regions by particle tracking (computational fluid dynamics (CFD) plot function)

The CFD plot function of HyperView allows one to generate streamlines using any available nodal vector field. The flow velocity streamlines are shown in Fig. 9, which represent the flow paths of nodal particles from the billet to the final extrudate. The distribution of metal streamlines in the die cavity stands for the velocity value of metal flow. More metal streamlines exist, metal flows faster. In addition, it is observed that dead regions exist with few streamlines at the bottom of the port bridge, the corner of the chamber and container, which illustrates that the metal in these regions seems not to participate in the deformation. This phenomenon is caused by the great frictional resistance that existed between material and container or die cavity under the conditions of nonlubricants in the extrusion process. Another reason maybe that results from the die structure leads to very high hydrostatic pressure at these local regions.

Furthermore, when the material encounters the baffle plates in the welding chamber, the metal will be forced to change the original direction and will flow into the region

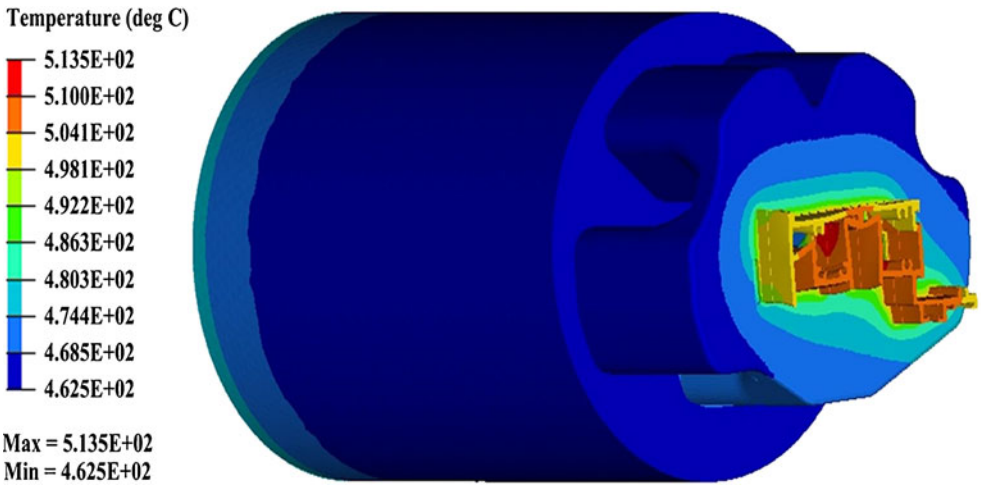

Fig. 11 Temperature distribution of whole numerical model

Fig. 12 Nose end of practical production

that is easy to form around baffle plates, which can balance the metal flow effectively as shown in Fig. 10.

3.3 Temperature evolution

In the extrusion process, the temperature evolution in the porthole die cavity is mainly influenced by heat transfer, frictional heat, and plastic deformation heat. Figure 11 shows the temperature distribution of the whole numerical model of the extrudate and it can be seen that the material temperature drops down at first then goes up along the extrusion direction. It is because the heat transfers from the billet to the die with lower temperature continuously, meanwhile the heat generated by the upsetting deformation cannot offset the heat loss to the porthole die at the beginning of the extrusion process, therefore the temperature of the billet drops down slightly with a minimum temperature of 462°C. Then the billet metal is split into distinct streams upon entering the mandrel of a porthole die, which can be considered as a multihole flat die extrusion process. From this moment on, plastic deformation is clearly greater than that at the early stage of extrusion process, thus the temperature goes up slightly, however the material temperature at this moment is still under the initial billet temperature. When the material flows into the welding chamber, the plastic deformation becomes greater and greater, and plastic deformation heat gradually surpasses that loses to the porthole die, as a result, the billet material temperature goes up continuously along the extrusion direction. When entering the die bearing, due to the maximum deformation occurring here, the material temperature reaches the peak of 513°C. From the above analysis, the temperature rise of extrudated material is mainly caused by plastic deformation heat during the extrusion process.

4 Experimental verifications and discussions

With the numerical solution, a real mold is manufactured and practical profile extrusion is accomplished. The process parameters used in the present finite element simulations and real production were exactly the same. It is difficult to obtain a good experimental verification of the numerical results. However, a rough comparison with the actual exit velocity can be obtained by looking at the nose end of the profile [4], which is often used to adjust die structure. This experimental nose end is shown in Fig. 12. The figure shows that the distribution in exit velocity has similar trend as the numerical result, and local regions (parts 2 and 3 in Fig. 7) with relative large deformation are also observed by experimental method. Based on these results, the adjustments of die structure, such as geometry and size of porthole, bearing length, etc., can be made to compensate for this velocity difference.

To validate the numerical method used in this work, another comparison between numerical and experimental nose ends for a different profile is carried out as shown in Fig. 13. A similar velocity distribution can also be observed by this comparison. Therefore, the numerical model built in this research could provide reasonable results and useful guidelines for practical production.

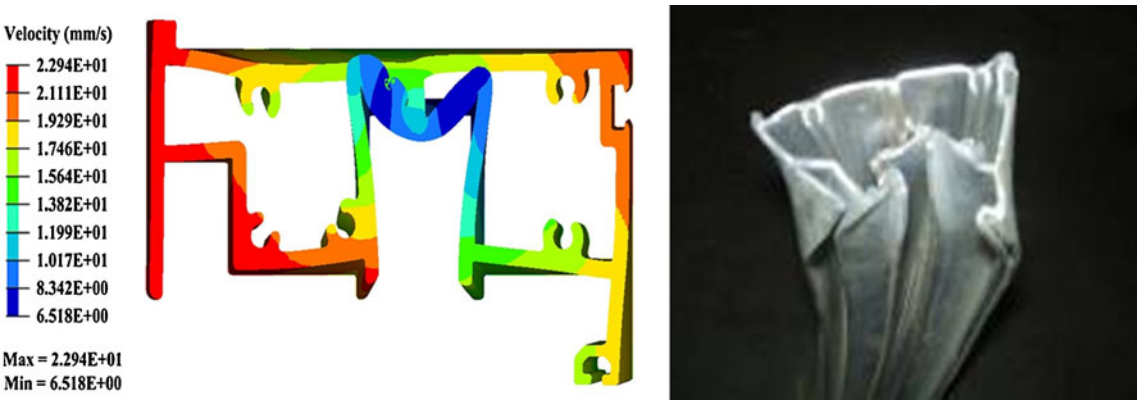

Fig. 13 Comparison between numerical and practical nose end for another case

5 Conclusions

This paper has described in detail the construction procedure of a numerical model for a complex hollow aluminum profile extrusion process with the commercial program HyperXtrude such as mesh size, boundary conditions, process parameters, etc. Meanwhile, metal flow behavior in the die cavity at every stage has been investigated. The conclusions have been drawn as follows:

1. The perfect agreement between numerical results and practical productions showed that numerical model developed in this paper could be used to investigate the metal flow, velocity or temperature distributions, and to optimize die design. Moreover, numerical method could partly replace the trial-and-error one in the real field of production to improve extrudate quality, enhance production capacity, and reduce production cost.
2. By means of particle tracking function provided by HyperXtrude, metal flow behavior at each stage during extrusion process has been investigated and dead zones in the die cavity could be clearly observed, which is convenient for further research of metal flow rules.
3. The final comparison with practical productions was only used to verify the numerical method. From the numerical and experimental results, due to the initial unreasonable die design, the velocity distribution at the cross-section of the extrudate was not perfect, which leads to twist deformation of the extrudate. In the following work, some adjustments or modifications of the die design will be made to balance the metal flow during the extrusion process.

Acknowledgments The authors would like to acknowledge financial support from the National Natural Science Foundation of China (51105230) and China Postdoctoral Science Foundation (20100481247), Shandong Postdoctoral Creative Foundation (201003078), Shandong Provincial Natural Science Foundation (Z2008F09), State Key Laboratory of Materials Processing and Die & Mould Technology (2011-P09), Program for Changjiang Scholars and Innovative Research Team in University of Ministry of Education of China (IRT0931), and the National Science & Technology Pillar Program in the 11th 5-year Plan Period of the People's Republic of China (2009BAG12A07-B01).

References

1. Karayel D (2008) Simulation of direct extrusion process and optimal design of technological parameters using FEM and artificial neural network. Key Eng Mater 367:185–192
2. Abrinia K, Makaremi M (2009) An analytical solution for the spread extrusion of shaped sections. Int J Adv Manuf Technol 41:670–676
3. Yang DY, Park K, Kang YS (2001) Integrated finite element simulation for the hot extrusion of complicated Al alloy profiles. J Mater Process Technol 111:25–30
4. Lof J, Blokhuis Y (2002) FEM simulations of the extrusion of complex thin-walled aluminium sections. J Mater Process Technol 122:344–354
5. Li Q, Harris C, Jolly MR. FEM investigations for practical extrusion issues—extrusion process for complex 3D geometries; pocket designs of die; transverse weld phenomenon. Proceedings of the Eighth International Aluminum Extrusion Technology Seminar (ET' 04), 18–21 May 2004, Wauconda
6. Lee JM, Kim BM, Kang CG (2005) Effects of chamber shapes of porthole die on elastic deformation and extrusion process in condenser tube extrusion. Mater Des 26:327–336
7. Wu XH, Zhao GQ, Luan YG, Ma XW (2006) Numerical simulation and die structure optimization of an aluminum rectangular hollow pipe extrusion process. Mater Sci Eng A 435–436:266–274
8. Kim SH, Chung SW, Padmanaban S (2006) Investigation of lubrication effect on the backward extrusion of thin-walled rectangular aluminum case with large aspect ratio. J Mater Process Technol 180:185–192
9. Liu G, Zhou J, Duszczyk J (2008) FE analysis of metal flow and weld seam formation in a porthole die during the extrusion of a magnesium alloy into a square tube and the effect of ram speed on weld strength. J Mater Process Technol 200:185–198
10. Fang G, Zhou J, Duszczyk J (2009) FEM simulation of aluminium extrusion through two-hole multi-step pocket dies. J Mater Process Technol 209:1891–1900
11. Fang G, Zhou J, Duszczyk J (2009) Extrusion of 7075 aluminium alloy through double-pocket dies to manufacture a complex profile. J Mater Process Technol 209:3050–3059
12. Bastani AF, Aukrust T, Skauvik I (2010) Study of flow balance and temperature evolution over multiple aluminum extrusion press cycles with HyperXtrude 9.0. Key Engineering Materials 424:257–264
13. Mihelic A, Stok B (1998) Tool design optimization in extrusion processes. Comput Struct 68:283–293
14. Ulysse P (1999) Optimal extrusion die design to achieve flow balance. Int J Mach Tools Manuf 39:1047–1064
15. Zou L, Xia JC, Wang XY, Hu GA (2003) Optimization of die profile for improving die life in the hot extrusion process. J Mater Process Technol 142:659–664
16. Byon SM, Hwang SM (2003) Die shape optimal design in cold and hot extrusion. J Mater Process Technol 138:316–324
17. Chen ZZ, Lou ZL, Ruan XY (2007) Finite volume simulation and mould optimization of aluminum profile extrusion. J Mater Process Technol 190:382–386
18. Kraft FR, Gunasekera S (2005) Conventional hot extrusion. In: Semiatin, SL (ed) ASM handbook, volume 14a. Metal working: bulk forming. pp 421–439
19. HyperXtrude 10.0 manual. Altair Engineering, Inc. http://www.tx.altair.com
20. Kim YT, Ikeda K, Murakami T (2002) Metal flow in porthole die extrusion of aluminium. J Mater Process Technol 121:107–115